

Coulomb focusing in intense field atomic processes

Thomas Brabec,^{1,3} Misha Yu. Ivanov,^{1,2} and Paul B. Corkum¹

¹National Research Council of Canada, M-23A, Ottawa, Ontario, Canada K1A 0R6

²Laboratoire de Chimie Théorique, Faculté des Sciences, Université de Sherbrooke, Québec, Canada J1K 2R1

³Abteilung für Quantenelektronik und Lasertechnik, Technische Universität Wien, Gußhausstrasse 27, A-1040 Wien, Austria

(Received 22 December 1995)

In the intense field (long-wavelength) limit, the oscillating motion of an electron wave packet leads to multiple passes by the scattering Coulomb center. The influence of the Coulomb focusing, in combination with multiple returns, focuses parts of the electron wave function, increasing the efficiency of such intense field processes as multiphoton double ionization. Our calculations show enhancement by more than an order of magnitude for multiphoton double ionization of He at 0.8 μm . [S1050-2947(96)50110-1]

PACS number(s): 32.80.Rm, 31.15.-p

In the long-wavelength limit, the core mechanism of many intense laser-atom or laser-ion interactions [1–4] is tunnel ionization followed by oscillations of the electron in the laser field. The oscillating electron can reencounter the parent ion more than once; see Fig. 1. The returning electron can be regarded as a built-in electron beam incident on the nucleus, with current densities greatly exceeding state-of-the-art electron beams. Our calculations demonstrate that the current density supplied by the returning electron is even higher than anticipated so far [2–4]. The observed increase results from the focusing effect of the Coulomb potential. Due to spreading most of the electron wave packet misses the nucleus at the first return; however, due to small deflections during the first (and higher) returns, a significant part of the wave packet is focused into an area close to the center of the parent ion.

The purpose of this Rapid Communication is twofold. First, we demonstrate the importance of Coulomb focusing for nonsequential double ionization [5–7]. Nonsequential ionization (NSI) is a process where two fundamental areas of atomic physics, namely, correlated single-photon two-electron ionization and multiphoton processes, merge. There exist two theoretical models for NSI, the “shake-off” model and the “recollision” model. The basis of the shake-off model [5] is that during tunnel ionization of the first electron [Fig. 1(a), departing arrow] the second electron is promoted to excited states from where it is efficiently ionized by the laser field. The basis of the recollision model [1,2,6] is that the second electron is collisionally ionized when the first electron revisits the parent ion [Fig. 1(a), returning arrow]. So far, the NSI rate predicted by the recollision model [2,6,8] has been too small. Our analysis shows that, for the case of helium, the double-ionization rate is increased by more than an order of magnitude due to Coulomb focusing in combination with multiple returns of the oscillating electron. Thus, the discrepancy between the theoretical calculations and experiments [7] on NSI is resolved.

The second purpose of this paper is to discuss more general implications of Coulomb focusing in intense laser fields. We show that higher-order returns can enhance the NSI mechanism in Ne^{8+} by two orders of magnitude, which can be important for recombination x-ray laser schemes. Coulomb focusing will affect other strong field processes, such

as high-harmonic generation (HHG) and hot above-threshold ionization (ATI) in atoms, collisional ionization, bremsstrahlung, and inverse bremsstrahlung (IB) in plasmas.

The theoretical approach used here to model NSI is an extension of that used in Ref. [2]. Ionization of the first electron is treated by using quantum-mechanical tunnel ionization models. The subsequent evolution of the ionized electron and the bound electron in the electric field is governed by classical equations. To emulate the evolution of the electron wave packet, a set of trajectories is launched with initial conditions taken from the wave function of the tunneling electron. Full quantum-mechanical calculations exceed the capacity of the fastest computers currently available, while one-dimensional two-electron quantum-mechanical calculations do not account for focusing and other three-dimensional effects.

Evolution of the two-electron system after the tunnel ionization of the first electron is determined by the classical equations of motion (in atomic units):

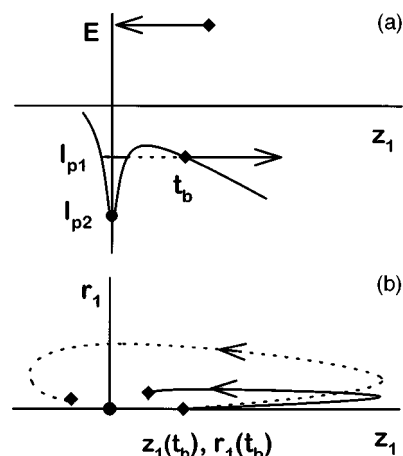


FIG. 1. Schematic of the evolution of a two-electron atom or ion in a strong laser field. The diamond represents the tunnel ionized electron; the circle represents the second (bound) electron. (a) Energy evolution of the first electron in time versus the z axis. The dotted line indicates tunneling with a rate w_{ion} ; t_b is the time of birth. (b) Space evolution of the first electron. The dotted line shows the Coulomb-focused trajectory.

$$\begin{aligned}\frac{d^2 r_i}{dt^2} &= -\frac{d}{dr_i}(V_{ne} + V_{ee}), \\ \frac{d^2 z_i}{dt^2} &= E_z(t) - \frac{d}{dz_i}(V_{ne} + V_{ee}).\end{aligned}\quad (1)$$

Here, r, z are cylindrical coordinates and $\mathbf{E}(t) = (0, 0, E_z \cos(\omega t))$ is the electric field. The indices $i = 1$ and 2 refer to the tunnel ionized and bound electron with ionization potentials I_{p1} and I_{p2} , respectively. The nucleus with charge q is modeled by a softened Coulomb potential [9], $V_{ne} = -q/(a^2 + r_i^2 + z_i^2)^{1/2}$. Softening improves quantitative agreement with quantum-mechanical calculations [9]. The parameter a is determined by the physical motivation that the Coulomb potential at the center is equal to the ionization potential I_{p2} . The electron-electron interaction is determined by the Coulomb potential $V_{ee} = 1/[(r_1 - r_2)^2 + (z_1 - z_2)^2]^{1/2}$.

The wave function of the tunneling electron at the time of birth t_b determines the initial conditions for the classical equations of motion [10]. The evolution of the wave packet is traced by launching a set of trajectories with different initial parameters t_b and v_{r1} , where v_{r1} is the initial velocity perpendicular to the polarization of the electric field. The weight of each classical trajectory in the ensemble is proportional to $w(t_b, v_r) = w_{ion}(t_b)w_r(v_{r1})$. Here, $w_{ion}(t_b)$ is the tunneling rate in the quasistatic approximation [11]. The quantum-mechanical transverse velocity distribution is [12] $w_r(v_{r1}) = 1/(\pi \delta v_{r1}^2) \exp[-(v_{r1}/\delta v_{r1})^2]$, where $\delta v_{r1} = (E_z/\sqrt{2I_p})^{1/2}$. The simulation range for the transverse velocity distribution is chosen as two times δv_{r1} and is divided into 60 000 equidistant trajectories. The results have been tested for numerical convergence by increasing the number of trajectories. The time t_b is varied over one optical half cycle. The remaining initial conditions for the first electron are $v_{z1}(t_b) = 0$, $r_1(t_b) = 0$, and z_1 is determined by the solution of the equation $zE_z(t_b) - V_{ne} = I_{p1}$ (see Fig. 1). The second electron is assumed to rest at the center of the model potential, i.e., $z_2 = r_2 = v_{r2} = v_{z2} = 0$.

To evaluate the probability for double ionization, Eq. (1) is solved in a time interval between t_b and $t_b + 15\pi/\omega$. During the last five half cycles the electric field is switched off using a \cos^2 envelope. Then, the double-ionization rate is determined by the integral $w_{di}(t_b) = \int_0^\infty dv_{r1} v_{r1} \theta(t_b, v_{r1}) w(t_b, v_{r1})$. The function $\theta(t_b, v_{r1})$ identifies the parameter ranges for which double ionization occurs, i.e., $\theta = 1$ when the kinetic energy of both electrons after the end of the laser pulse is greater than zero and $\theta = 0$ elsewhere.

Before studying the double-ionization problem we confirm the validity of our classical approach by calculating the field-free impact ionization cross section of $\text{He}^+ + e^- \rightarrow \text{He}^{2+} + 2e^-$. The parameters are $I_{p1} = 0.9$ a.u. (24.12 eV), $I_{p2} = 2$ a.u. (54.4 eV), and $a = 1$ a.u. Numerical results and experimental data [13] are in reasonable agreement; see Fig. 2(a).

A schematic of the evolution of the two electrons of He in the laser field is shown in Fig. 1. The tunneling electron is born on the outer edge of the barrier at the initial-state binding energy [8]. The complete set of trajectories representing

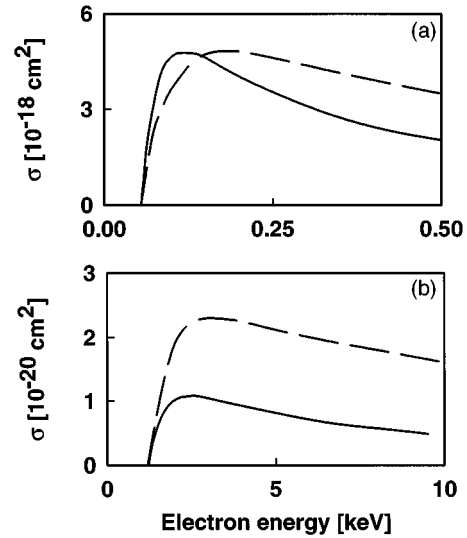


FIG. 2. Field-free impact ionization cross section σ for the processes (a) $e^- + \text{He}^+ \rightarrow 2e^- + \text{He}^{2+}$ and (b) $e^- + \text{Ne}^{8+} \rightarrow 2e^- + \text{Ne}^{9+}$. The full and dotted lines denote numerical results and experimental data of Ref. [13], respectively.

the evolution of the ionized electron in the laser field is very complex. Therefore, in Fig. 1 we have chosen two trajectories that illustrate the effect of Coulomb focusing on the evolution of the wave packet. During the periodic motion the electron can revisit the parent ion. For small impact parameters [Fig. 1(b), solid line] the electron interacts strongly with the ion to collisionally excite or ionize the bound electron during its first return. However, only a small fraction of the trajectories with low initial transverse velocities pass close enough to the nucleus to contribute to double ionization. Electrons with large impact parameters miss the nucleus at the first return. Due to small deflections during each encounter these trajectories can be focused into the double-ionization cross section after multiple returns [Fig. 1(b), dotted line]. Thus, the part of the wave function that contributes to nonsequential double ionization is considerably increased. This can be seen in Fig. 3, where the ionization rate $w_{di}(t_b)$ is depicted versus the phase of the laser field at the time of birth; laser wavelength is $\lambda = 780$ nm, and the electric field strength is $E_z = 0.169$ a.u. ($I = 1$ PW/cm²). At this intensity the tunneling probability of the second electron is small and the ionization rate is determined by the nonsequential process. The open diamonds and the lower shelf of the curve indicate the contribution to double ionization coming from the first recollision. The nonsequential ionization rate is increased by a factor of 30 due to higher returns. This factor is characteristic of intensities in the tunneling regime. The main contribution to double ionization comes from the plateau region close to the peak of the electric field. There, tunnel ionization is most efficient and electrons are born with low drift velocity so that higher-order returns are possible. The calculations show that the enhanced nonsequential ionization comes from trajectories with initial transverse velocities $< \delta v_{r1}/2$ that pass the nucleus at a distance between 5 a.u. (2.5 Å) and 20 a.u. (10 Å) during the first return. For trajectories with initial velocities well within the $1/e$ width, the velocity distribution does not sensitively depend on δv_{r1} , and small changes to the initial width of the wave

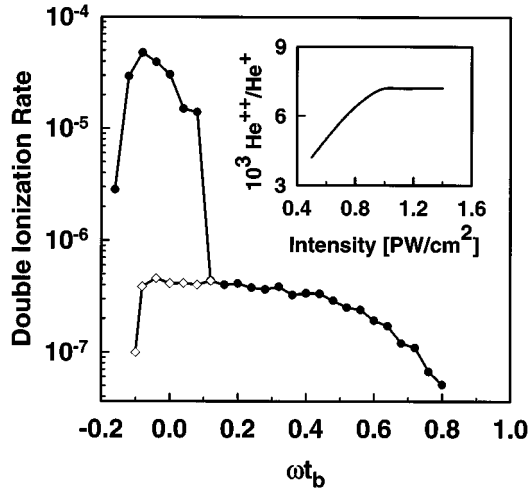


FIG. 3. NSI rate $w_{di}(t_b)$ for double ionization in He versus the phase of the laser field ωt_b at the moment of birth. The laser intensity is 1 PW/cm^2 . Inset: Relative ion yield $\text{He}^{2+}/\text{He}^+$ averaged over one laser cycle, versus laser intensity.

packet do not critically influence the double-ionization rate. For phases $\omega t_b > 0.16$ and $\omega t_b < -0.16$ classical Eqs. (1), in combination with initial conditions, do not allow for higher order returns.

Double ionization can take place when a trajectory is focused into an area close to the nucleus. The second important parameter determining the NSI rate is the energy of the returning electron. Calculations have shown that nonsequential ionization works efficiently when the bound electron is either knocked out by the returning electron or excited above the field-suppressed barrier $I_{p2}^* = I_{p2} - 2\sqrt{qE_z}$. The barrier suppression changes with the electric field and is strongest at the maximum of the electric field, E_z . Even when the barrier is not strongly suppressed at the time of excitation, the excited electron is ionized at the time of maximum barrier suppression during the next quarter cycle. We have found that double ionization can also occur when the kinetic energy supplied by the returning electron is less than I_{p2}^* . In this case the energy is gained by laser-assisted collision with the core. This mechanism gains importance with decreasing laser intensity. In quantum language, at lower intensities ionization proceeds via intermediate doubly excited states created during the recollision of the returning electron with the core.

The inset in Fig. 3 shows the double-ionization rate normalized to the tunnel ionization rate versus the laser intensity. The ionization rates have been averaged over one optical cycle. We have chosen the intensity range $I > 0.5 \text{ PW/cm}^2$, where the Keldysh parameter $\gamma = \omega\sqrt{I_p}/E_z \approx < 0.5$ and ionization is dominated by tunneling. Due to the strong nonlinearity of tunnel ionization the peak intensity determines the nonsequential double ionization rate, and the data plotted in the inset in Fig. 3 are rather insensitive to pulse parameters. Inclusion of the pulse parameters of Ref. [7] reduces the double-ionization rate by 20%. Qualitatively, our calculations agree with the experimental data presented in Fig. 3 of Ref. [7]. Quantitatively, we calculate an ionization rate three times too high. In general, we expect classical calculations to overestimate the double-ionization rate for

two reasons. First, the classical model has a continuum of bound states. In our case this is not a severe overestimate, since in the barrier-suppressed region, where double ionization is most effective, the electronic states form a quasicon- tinuum. Second, excitation to low-energy continuum levels is overestimated by our classical model, as can be seen from Fig. 2(a).

In the remainder of the paper we discuss the implications of nonsequential ionization on the generation of multiply charged ions. One application of NSI at reduced intensities might be recombination x-ray lasers; see, e.g., Ref. [14]. Consider, as an example, a neon atom in a laser field with parameters similar to those used in two recent experiments [15]: $\lambda = 250 \text{ nm}$, $E_z = 2.38 \text{ a.u.}$ ($I = 200 \text{ PW/cm}^2$). The smoothing parameter is $a^2 = 0.0419$. For the calculation it is assumed that the first seven electrons have been field ionized. The remaining Ne^{7+} ion is approximated by the two-electron model used above. The first electron is tunnel ionized from the $2s^1$ state with $I_{p1} = 8.79 \text{ a.u.}$ (239.1 eV). The second electron is bound in the $1s^2$ state with $I_{p2} = 43.96 \text{ a.u.}$ (1195.8 eV).

As before, we first test the applicability of the model atom by calculating the impact ionization cross section $\text{Ne}^{8+} + e^- \rightarrow \text{Ne}^{9+} + 2e^-$. The numerical results show reasonable agreement with experimental data [13]; see Fig. 2(b). The overall difference of a factor of 2 is likely the result of approximating the two bound electrons by one electron. Repeating the same calculation as performed for He we obtain the relative number of ions averaged over one optical cycle, $\text{Ne}^{9+}/\text{Ne}^{8+} = 3 \times 10^{-4}$. Taking into account only the contributions from the first return yields $\text{Ne}^{9+}/\text{Ne}^{8+} \approx 3 \times 10^{-6}$. The absolute ionization probability per laser cycle ($\approx 1 \text{ fs}$) for Ne^{9+} is $\approx 10^{-5}$.

In the experiment of Lee *et al.* [15] the fluorescence of various species of ionized noble gases has been measured. Although core vacancies in the 1-keV range (Xe^{11+} , Ne^{9+}) have been observed experimentally [15], no immediate relaxation radiation has been found. Our qualitative results are completely consistent with these data. At intensities greater than 100 PW/cm^2 , all excited states of studied ions are above the field-suppressed barrier and are immediately ionized. Therefore, no prompt radiation coming from a field-assisted collisionally excited core vacancy should be observed.

Finally, Coulomb focusing is important for other areas of strong-field physics. In atomic physics, NSI, high-harmonic generation, and hot above-threshold ionization are based on the same physical mechanism [2]. A tunnel [16] ionized electron is accelerated in the electric field and interacts with the parent ion during subsequent recollisions. Therefore, Coulomb focusing must make a significant contribution from high-order returns to ATI. Similarly, the single-atom dipole moment—the source term for HHG—will be increased. However, experiments on HHG are influenced by propagation effects as well. Whether the more complicated phase structure of the dipole moment for higher-order returns in combination with the accumulation of the phase during propagation will result in the suppression of the contribution from high-order returns requires further study.

Plasma processes, such as bremsstrahlung, inverse bremsstrahlung, and collisional ionization in laser fields, are

closely related to ATI and NSI. If the drift (thermal) energy of the electron is smaller than the quiver energy, focusing of electrons in the combined action of the electric field and the Coulomb potential makes several encounters possible. This will lead to corrections to current theories [17].

We have only considered interaction with a single ion. For plasma applications often a high gas density is desirable. With increasing density, interactions with other electrons or neighbor ions have to be taken into account. These interactions perturb the focusing of the electron trajectories and weaken the enhancement of the nonsequential ionization rate. A conservative estimate for the density at which the effect of adjacent ions becomes relevant can be obtained by comparing the average distance between the ions d_a with the

amplitude of the electron oscillation in the electric field $a_q = 2E_z/\omega^2$. For the parameters used above $a_q = 150$ a.u (8 nm) and $d_a \approx a_q$ for a density of $2 \times 10^{18} \text{ cm}^{-3}$. Many plasma experiments, including those of Ref. [15], fall within this low-density range. Electron-electron collisions become relevant at significantly higher densities and are not considered here.

We acknowledge very helpful discussions with N. H. Burnett. This work was partially supported by the Österreichische Nationalbank Jubiläumsfondprojekt No. 5124. T. Brabec is supported by the Österreichische Akademie der Wissenschaften, APART Grant. M. Yu. Ivanov is supported by an NSERC collaborative research grant.

-
- [1] M. Yu. Kuchiev, Pis'ma Zh. Eksp. Teor. Fiz. **45**, 319 (1987) [JETP Lett. **45**, 404 (1987)]; I. L. Beigman and B. N. Chickov, *ibid.* **46**, 399 (1987).
 - [2] P. B. Corkum, Phys. Rev. Lett. **71**, 1994 (1993).
 - [3] K. J. Schafer *et al.*, Phys. Rev. Lett. **70**, 1599 (1993).
 - [4] M. Lewenstein *et al.*, Phys. Rev. A **49**, 2117 (1994); W. Becker, S. Long, and J. K. McIver, *ibid.* **50**, 1540 (1994).
 - [5] D. N. Fittinghoff *et al.*, Phys. Rev. Lett. **69**, 2642 (1992).
 - [6] P. Dietrich *et al.*, Phys. Rev. A **50**, R2585 (1994); S. Augst *et al.*, *ibid.* **52**, R917 (1995).
 - [7] B. Walker *et al.*, Phys. Rev. Lett. **73**, 1227 (1994).
 - [8] K. C. Kulander, J. Cooper, and K. J. Schafer, Phys. Rev. A **51**, 561 (1995).
 - [9] M. Gajda *et al.*, Phys. Rev. Lett. **46**, 1638 (1992); Q. Su, J. H. Eberly, and J. Javanainen, *ibid.* **64**, 862 (1990).
 - [10] This approach accounts for the spreading of the electron wave packet, but, similar to the geometrical limit of optics, does not include phase (interference) effects.
 - [11] A. M. Perelomov, V. S. Popov, and V. M. Teren'ev, Zh. Eksp. Teor. Fiz. **50**, 1393 (1966) [Sov. Phys. JETP **23**, 924 (1966)]; M. V. Ammosov, N. B. Delone, and V. P. Krainov, *ibid.* **91**, 2008 (1986) [*ibid.* **64**, 1191 (1986)].
 - [12] N. B. Delone and V. P. Krainov, J. Opt. Soc. Am. B **8**, 1207 (1991).
 - [13] H. Tawara and T. Kato, At. Data Nucl. Data Tables **36**, 167 (1987).
 - [14] N. H. Burnett and G. D. Enright, IEEE J. Quantum Electron. **26**, 1797 (1990).
 - [15] W. J. Blyth *et al.*, Phys. Rev. Lett. **74**, 554 (1995); P. H. Y. Lee, D. E. Casperson, and G. T. Schappert, Phys. Rev. A **40**, 1363 (1989).
 - [16] M. Lewenstein, K. C. Kulander, K. J. Schafer, and P. H. Bucksbaum, Phys. Rev. A **51**, 1495 (1995).
 - [17] See review by L. Schlessinger and J. Wright, Phys. Rev. A **20**, 1934 (1979).